Heliyon 10 (2024) e26487

Contents lists available at ScienceDirect

Heliyon

journal homepage: www.cell.com/heliyon

Research article

Optimal control and cost-effectiveness analysis for the human melioidosis model

Habtamu Ayalew Engida [a,*], Duncan Kioi Gathungu [b], Melkamu Molla Ferede [c], Malede Atnaw Belay [d], Patiene Chouop Kawe [b], Bilali Mataru [e]

[a] Department of Applied Mathematics, Debre Markos University, P.O. Box 269, Debre Markos, Ethiopia
[b] Department of Mathematics, Jomo Kenyatta University of Agriculture and Technology, P.O. Box 62000-00200 City Square, Nairobi, Kenya
[c] Department of Statistics, University of Gondar, P.O. Box 196, Gondar, Ethiopia
[d] Department of Applied Mathematics, University of Gondar, P.O. Box 196, Gondar, Ethiopia
[e] Muslim University of Morogoro, Tanzania

ARTICLE INFO

Keywords:
Melioidosis
Burkholderia pseudomallei
Optimal control
Numerical simulation
Cost-effectiveness

ABSTRACT

In this work, we formulated and investigated an optimal control problem of the melioidosis epidemic to explain the effectiveness of time-dependent control functions in controlling the spread of the epidemic. The basic reproduction number (R_{0c}) with control measures is obtained, using the next-generation matrix approach and the impact of the controls on R_{0c} is illustrated numerically. The optimal control problem is analyzed using Pontryagin's maximum principle to derive the optimality system. The optimality system is simulated using the forward-backward sweep method based on the fourth-order Runge-Kutta method in the MATLAB program to illustrate the impact of all the possible combinations of the control interventions on the transmission dynamics of the disease. The numerical results indicate that among strategies considered, strategy C is shown to be the most effective in reducing the number of infectious classes compared to both strategy A and strategy B. Furthermore, we carried out a cost-effectiveness analysis to determine the most cost-effective strategy and the result indicated that the strategy B (treatment control strategy) should be recommended to mitigate the spread and impact of the disease regarding the costs of the strategies.

1. Introduction

Melioidosis is an emerging infectious disease caused by the environmental gram-negative bacterium called *Burkholderia pseudomallei* [4,14,30]. This bacterium is commonly found in moist soil and surface water in tropical and subtropical regions, particularly in Southeast Asia, Northern Australia and sub-Saharan Africa [10,21,28]. The disease can affect both humans and animals. Humans acquire infection through ingestion, inoculation and inhalation of the bacteria from contaminated soil or water [10,11,28]. Human-to-human transmission is usually uncommon, with only a small number of suspected cases documented to date, which oc-

* Corresponding author.
E-mail addresses: hayalew21@gmail.com (H.A. Engida), dkioi@jkuat.ac.ke (D.K. Gathungu), melkamum2m@gmail.com (M.M. Ferede), atnawmalede1982@gmail.com (M.A. Belay), patiene@aims-cameroon.org (P.C. Kawe), bilalimataru@mum.ac.tz (B. Mataru).

https://doi.org/10.1016/j.heliyon.2024.e26487
Received 17 May 2023; Received in revised form 9 February 2024; Accepted 14 February 2024

Available online 21 February 2024

curred through contact with the reproductive fluid of an infected human or breastfeeding from an infected mother [7,9,14,36,41]. According to recent studies, *B. pseudomallei* causes approximately 165,000 human infections and 89,000 (54%) fatalities per year throughout the world [14,27,47].

Melioidosis is a serious infection in humans and it can cause a wide range of symptoms, from mild flu-like illness to severe sepsis and pneumonia. The symptoms may include fever, headache, muscle aches, joint pain, cough, chest pain, difficulty breathing, and skin lesions. In severe cases, the infection can lead to septic shock, multiple organ failure, and death [9,13,14,22].

Subsequent studies have indicated the effectiveness of a two-stage antibiotic treatment for melioidosis, consisting of an initial phase (the acute phase) of intravenous antibiotics followed by a subsequent phase (the eradication phase) of oral drug. In the acute phase, the current antibiotic options are ceftazidime and carbapenem, and the treatment with these antibiotics should continue for a duration longer than 2 weeks. While oral trimethoprim-sulfamethoxazole (TMP-SMX) is the antibiotic choice during the subsequent eradication phase for 13-26 weeks [10,12,16,41]. However, *B. pseudomallei* species are intrinsically resistant to several classes of antimicrobial agents and some isolates are also resistant to the two-phase antibiotics [16,39]. In addition, the disease infection relapse varies from 13% to 23% in patients [39]. The reasons for infection relapse are antimicrobial resistance (severity of *B. pseudomallei*), inadequate or incomplete antimicrobial agents and improper eradication therapy among others [23,39]. To date, there is no vaccine for human melioidosis [29]. Prevention measures involve avoiding contact with contaminated soil or water, wearing protective clothing and footwear when working in high-risk environments, treating drinking water and practising good personal hygiene [8,41].

Mathematical modeling has shown its significant role in the study of epidemiology by providing more insight into the underlying mechanisms for preventing and controlling infectious diseases [19,20]. Nowadays, optimal control theory plays a critical role in showcasing the effectiveness of various optimal control interventions for a given mathematical model through the incorporation of suitable control measures [26,40]. A few researchers have proposed autonomous compartmental mathematical models to address the transmission dynamics of the disease, see literature [29,45]. The authors in [29] presented a susceptible-exposed-infected-recovered-susceptible (SEIRS) deterministic model to show key factors of the disease incidence pattern in Thailand. The authors in [45] proposed a susceptible-exposed-infected-recovered (SEIR) model of the melioidosis epidemic to address the dynamics behavior of the disease in the human population. Also, the author in [44] considered a SEIR compartmental model to achieve the effectiveness of hygiene care and treatment control factors on the transmission process of melioidosis. Recently, the authors in [14] developed a susceptible-exposed-asymptomatic infectious-symptomatic infectious-recovered-susceptible (SEAIRS) deterministic model that describes the transmission dynamics of human melioidosis with an asymptomatic class. They presented a detailed stability analysis of the steady states of their model qualitatively and quantitatively. They also demonstrated the impact of model parameters on disease dynamics. They further carried out numerical experiments to support their theoretical results.

In this paper, we propose an optimal control problem for the dynamics of human melioidosis, which is a continuation of the research started in [14]. This work aims to demonstrate the effectiveness and cost-effectiveness of optimal control interventions in controlling the spreading of the epidemic.

The rest of the paper is divided into the following Sections: we describe the basic model from the study [14] in Section 2. The formulation of an optimal control problem and characterization of the optimal control problem are described in Section 3. Numerical simulations of different control interventions and their cost-effectiveness analysis are carried out in Section 4. The concluding results are given in Section 5.

2. The autonomous model

The state system is an autonomous system of non-linear ordinary differential equations from the model formulated in [14]. The model divides the total human (host) population at time t, into five distinct compartments: susceptible class ($S(t)$), latently-infected class ($E(t)$), asymptomatic class (infectious individuals without symptoms and can transmit the disease) ($A(t)$), symptomatic class (infectious individuals that are showing symptoms and can transmit the disease to others) ($I(t)$), and recovered class ($R(t)$), where, the total population is given by $N(t) = S(t) + E(t) + A(t) + I(t) + R(t)$. The concentration of *B. pseudomallei* in the environment at time t, is denoted by $B_m(t)$. The susceptible class is assumed to increase due to newborns at a constant recruitment rate given by Π. Susceptible humans may be infected through either contact with bacterial class at the rate $\beta_1 \frac{B_m}{C+B_m}$, or contact with infectious classes $\left(A(t)\&I(t)\right)$ at the rate $\beta_2(I + \sigma A)$, where β_1 and β_2, respectively, are transmission rates due to the pathogen and infectious individuals, C is the constant pathogen concentration in the environment that yields 50% chance of catching the disease, and σ is the reduction rate in infectivity of A with, $0 < \sigma < 1$. The number of susceptible humans infected by *B. pseudomallei* due to the contaminated environment per unit time is given by $\beta_1 \frac{B_m}{C+B_m} S$, while the number of susceptible humans infected by *B. pseudomallei* due to $A(t)$ and $I(t)$ per unit time is given by $\beta_2(I + \sigma A)S$. Hence, the number of susceptible humans infected by melioidosis per unit of time is given by $\left(\beta_1 \frac{B_m}{C+B_m} + \beta_2(I + \sigma A)\right)S$ and joins E. The rate at which individuals in E progress to I is denoted by θ, while the individuals in E progress to A at the rate of $(1 - \theta)$. The shedding rate of *B. pseudomallei* into the environment due to A and I is given by η. The respective human and bacterial natural death rates are represented by μ and μ_b. The disease-induced death rate is denoted as δ. The recovery rate from A is denoted by γ_1 while from I is denoted by γ_2. The individuals in R progress to S at the rate of α. Moreover, the description, values and sources of the model parameters are given in Table 1. The autonomous system of the model from [14] is given as

$$\begin{cases} \frac{dS}{dt} = \Pi + \alpha R - (\lambda + \mu)S, \\ \frac{dE}{dt} = \lambda S - (\rho + \mu)E, \\ \frac{dA}{dt} = (1-\theta)\rho E - (\delta + \gamma_1 + \mu)A, \\ \frac{dI}{dt} = \theta\rho E - (\delta + \gamma_2 + \mu)I, \\ \frac{dR}{dt} = \gamma_1 A + \gamma_2 I - (\alpha + \mu)R, \\ \frac{dB_m}{dt} = \eta(A + I) - \mu_b B_m, \end{cases} \tag{1}$$

where, $\lambda = \beta_1 \frac{B_m}{C+B_m} + \beta_2(I + \sigma A)$, with the initial conditions;

$$S(0) = S_0 > 0,\ E(0) = E_0 > 0,\ A(0) = A_0 > 0,\ I(0) = I_0 > 0,\ R(0) = R_0 \geq 0,\ B_m(0) = B_{m,0} > 0.$$

For the model equation (1), stability analysis and sensitivity analysis were carried out, and the non-negativity and boundedness of the solution components of such system was established in [14]. Also, the basic reproduction number (R_0) of the model is given as (see, in [14])

$$R_0 = \Pi\rho\left(\frac{\beta_1\eta(\theta\epsilon_1 + (1-\theta)\epsilon_2) + C\mu_b\beta_2(\theta\epsilon_1 + \sigma(1-\theta)\epsilon_2)}{(\rho+\mu)C\mu\mu_b\epsilon_1\epsilon_2}\right) = R_{0h} + R_{0b}$$

where,

$$R_{0h} = \frac{\Pi\rho\beta_2\left[\theta(\delta+\gamma_1+\mu) + \sigma(1-\theta)(\delta+\gamma_2+\mu)\right]}{\mu(\rho+\mu)(\delta+\gamma_1+\mu)(\delta+\gamma_2+\mu)},$$

is the basic reproduction number due to human-to-human transmission, and

$$R_{0b} = \frac{\Pi\rho\beta_1\left[\theta(\delta+\gamma_1+\mu) + (1-\theta)(\delta+\gamma_2+\mu)\right]}{C\mu\mu_b(\rho+\mu)(\delta+\gamma_1+\mu)(\delta+\gamma_2+\mu)},$$

is the basic reproduction number due to environment-to-human transmission. R_0 measures the average number of secondary infectious individuals generated by a single infected person (asymptomatic or symptomatic) in completely susceptible humans.

By using the approach given in [14] and the parameter values from Table 1, the most influencing parameter of the model are human recruitment rate (Π) followed by the transmission rate due to infectious humans (β_2), the transmission rate due to the environment (β_1) mortality rate of bacteria (μ_b) and recovery rates (γ_2 & γ_1), respectively. This indicates that a personal preventive intervention for susceptible humans and control intervention of the transmission rate (β_1) will sufficiently diminish the spread of the disease. Also, control strategies that increase the natural mortality rates of bacteria or a strategy that increases the recovery rates of infectious humans would be effective in diminishing the spread of the epidemic.

This paper transforms an autonomous mathematical model without controls into a non-autonomous model with controls by incorporating two bounded control functions of time, which affect the value of R_0 and the effect of these control functions on it is demonstrated in section 3.1. Therefore, to use optimal efforts on interventions to eliminate the disease from the infected population, an optimal control problem of melioidosis with cost-effectiveness analysis is discussed in this study.

3. Analysis of the optimal control model

In this section, we formulate an optimal control problem to investigate the effect of two time-dependent preventive and control measures on the transmission dynamics of melioidosis. These time-dependent measures are introduced at a specified time $t \in [0, T]$ as follows, where T is the final time;

(i): $u_1(t)$ the preventive measure applied on susceptible class: using appropriate personal protective equipment (wearing rubber boots, rubber gloves or waterproof dressings to cover wounds or skin) and using treated water for drinking; this is to minimize the acquisition of the infection in the population.

(ii): $u_2(t)$ the treatment control measure implemented on infectious classes; this is to reduce the number of infectious individuals in the population. The disease infection can be treated by intravenous antibiotics including ceftazidime, imipenem, or meropenem for a minimum of 10-14 days, followed by oral trimethoprim-sulfamethoxazole (TMP-SMX) drug for 3-6 months [16,29,39].

The melioidosis non-autonomous model with the time-dependent measures is formulated as;

$$\begin{cases} \frac{dS}{dt} = \Pi + \alpha R - \left((1-u_1)\beta_1 \frac{B_m}{C+B_m} + \beta_2(I+\sigma A) + \mu\right) S, \\ \frac{dE}{dt} = (1-u_1)\beta_1 \frac{B_m}{C+B_m} S + \beta_2(I+\sigma A)S - (\rho+\mu)E, \\ \frac{dA}{dt} = (1-\theta)\rho E - (\delta+\gamma_1+\xi u_2+\mu)A, \\ \frac{dI}{dt} = \theta\rho E - (\delta+\gamma_2+\xi u_2+\mu)I, \\ \frac{dR}{dt} = (\gamma_1+\xi u_2)A + (\gamma_2+\xi u_2)I - (\alpha+\mu)R, \\ \frac{dB_m}{dt} = \eta(A+I) - \mu_b B_m. \end{cases} \tag{2}$$

The constant coefficient ξ is the control rate of treatment. The incidence rate of infection due environment-to-human interaction diminished by the factors $(1-u_1(t))$ and infectious classes is minimized at the rate of $\xi u_2(t)$. Next, we need to formulate an appropriate objective function for the state system (2). This study is aimed to reduce the size of infectious classes and the associated cost of the interventions over the specified time interval. Thus, the form of the objective functional, J, to be minimized is given by:

$$J(u_1,u_2) = \int_0^T \left(w_1 A + w_2 I + \frac{w_3}{2}u_1^2 + \frac{w_4}{2}u_2^2\right) dt \tag{3}$$

subject to the model equation (2). We consider the quadratic forms of the cost control functions in the objective functional $J(u_1,u_2)$. The nonlinear nature of the cost of intervention arises based on the fact that there is no linear relationship between the effects of interventions and their costs in the infected population. See for more details in some related literature [3,24,33,35,42]. w_k are the positive balancing weight constants, for k = 1, 2. The terms w_1A and w_2I, respectively, in the objective cost functional J are the costs associated with asymptomatic infectious individuals and symptomatic infectious individuals that need to be minimized. The expressions $\frac{w_3}{2}u_1^2$ and $\frac{w_4}{2}u_2^2$ represent the cost associated with prevention and treatment control measures, respectively. Since the formulated optimal control problem is aimed to minimize the number of infectious individuals under minimum cost, we seek the optimal control pair $u_1^*(t)$ and $u_2^*(t)$) such that

$$J(u_1^*,u_2^*) = \min_{u_k \in U}\{J(u_1,u_2)\}, \text{ where } k = 1,2, \tag{4}$$

where, U is a non-empty bounded admissible control set described by

$$U = \{\left(u_1(t),u_2(t)\right) : 0 \le u_k \le 1, \text{ each } u_k \text{ is Lebesgue measurable, for } k = 1,2,\ t \in [0,T]\}.$$

3.1. The effects of the control variables (u_1 & u_2) on basic reproduction number of the system (2)

This section presents the effects of the control variables, u_1 and u_2, on the basic reproduction number (denoted by R_{0c}) of the non-autonomous system (2). To obtain R_{0c} of the system (2), the next-generation matrix approach [46] is used as follows. The associated Jacobian matrices of the new infection terms F and the rate of transfer of individuals to the compartments V are given by:

$$F = \begin{pmatrix} 0 & \frac{\beta_2\sigma\Pi}{\mu} & \frac{\beta_2\Pi}{\mu} & (1-u_1)\frac{\beta_1\Pi}{C\mu} \\ 0 & 0 & 0 & 0 \\ 0 & 0 & 0 & 0 \\ 0 & 0 & 0 & 0 \end{pmatrix} \text{ and } V = \begin{pmatrix} \rho+\mu & 0 & 0 & 0 \\ -(1-\theta)\rho & (\delta+\gamma_1+\xi u_2+\mu) & 0 & 0 \\ -\theta\rho & 0 & (\delta+\gamma_2+\xi u_2+\mu) & 0 \\ 0 & -\eta & -\eta & \mu_b \end{pmatrix}.$$

Thus, R_{0c} of the system (2) given by

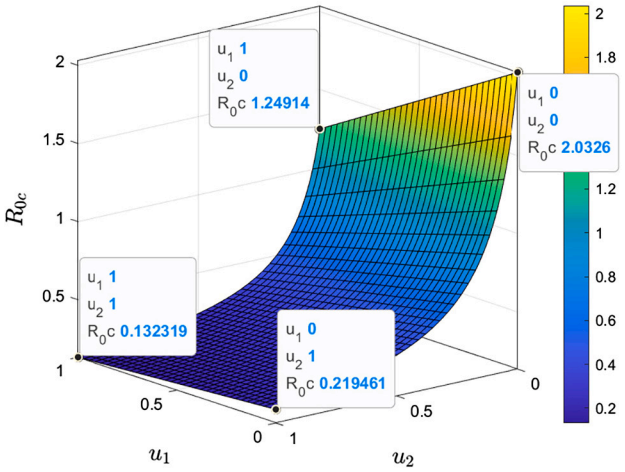

Fig. 1. Plot showing the effects of u_1 & u_2 on R_{0c} for $0 \le u_1 \le 1, 0 \le u_2 \le 1$. The parameter values given in Table 1 are used.

$$R_{0c} = \rho(FV^{-1}) = \Pi\rho\left(\frac{(1-u_1)\beta_1\eta\Big(\theta\epsilon_1 + (1-\theta)\varepsilon_2\Big) + C\mu_b\beta_2\Big(\theta\epsilon_1 + \sigma(1-\theta)\varepsilon_2\Big)}{(\rho+\mu)C\mu\mu_b\epsilon_1\epsilon_2}\right),$$

where, $\epsilon_1 = \delta + \gamma_1 + \xi u_2 + \mu$, $\epsilon_2 = \delta + \gamma_2 + \xi u_2 + \mu$.

The variation of R_{0c} with respect to the controls is depicted in surface plot (see, Fig. 1) for $0 \le u_1 \le 1, 0 \le u_2 \le 1$. A similar approach can be found in [25]. The Fig. 1 indicates that the highest value of R_{0c} is achieved when both control variables are at their minimum value, $u_1 = u_2 = 0$. This value, $R_{0c} = 2.0326$, corresponds to the basic reproduction number (R_0) of autonomous system (1). Another higher value of R_{0c} ($1.29914 > 1$) is obtained when $u_1 = 1$ and $u_2 = 0$, which suggests that implementing the preventive measure u_1 alone is not effective in eradicating the melioidosis epidemic. On the other hand, when both controls, u_1 and u_2 are set to their maximum values (i.e. full efforts), the minimum value of R_{0c} is achieved, which is 0.13239 as depicted in Fig. 1. This indicates that the combination of both control measures is highly effective in reducing R_{0c}. The results suggest that the control strategy involving the use of both u_1 and u_2 can lead to the complete elimination of the disease from the infected population. Moreover, when only u_2 is used at full effort ($u_2 = 1$) while u_1 is absent ($u_1 = 0$), a lower value of R_{0c} is observed, which is 0.219461. This value is less than unity, suggesting that the treatment control measure u_2 alone is also effective for eradicating the disease. Consequently, a strategy of the combination of both control measures (u_1 and u_2) as well as a strategy involving treatment control only would be effective in reducing the spread of the disease within the community. Furthermore, the effectiveness and cost-effectiveness of these control functions are discussed in the numerical simulation section.

3.2. Existence of an optimal control

Theorem 3.1. *Given the objective functional J, defined on the control set U, and subject to the non-autonomous system (2), then there exists an optimal control pair $u = (u_1^*, u_2^*)$ such that the equation (4) holds, provided that the following conditions are hold [15,17,32,34]:*

(i) *The control set is closed and convex.*
(ii) *The right hand-side of the state system (2) is bounded by a linear function in the state and control variables.*
(iii) *The integrand of the objective functional in the equation (3) is convex with respect to the controls.*
(iv) *There exist constants $\alpha_1, \alpha_2 > 0$ and $\alpha_3 > 1$ such that the integrand of the objective functional is bounded below by*

$$\alpha_1\left(\sum_{k=1}^{2} |\, u_k \,|\right)^{\frac{\alpha_3}{2}} - \alpha_2.$$

Proof. We need to verify the four hypotheses stated by Theorem 3.1.

(i) Given the control set $U_0 = \{(u_1, u_2) : 0 \le u_1 \le 1, 0 \le u_2 \le 1\}$. Then, U_0 is closed by definition. Further, let a and b be any two arbitrary points in U_0, such that $a = (a_1, a_2)$ and $b = (b_1, b_2)$. From the concept of convex set [43], it follows that

$$\phi a_k + (1-\phi)b_k \in [0,1], \ \forall \phi \in [0,1], \ k = 1, 2.$$

This implies, $\phi a + (1-\phi)b \in U_0$. Thus, U_0 is convex set.

(ii) Let $x = (S, E, A, I, R, B_m)$ be the state variables of the model, $u = (u_1, u_2) \in U_0$ and $f(t, x, u)$ be the right-hand side of the system (2) given by

$$f(t,x,u)=\begin{bmatrix}\Pi+\alpha R-\left((1-u_1)\beta_1\frac{B_m}{C+B_m}+\beta_2(I+\sigma A)+\mu\right)S\\(1-u_1)\beta_1\frac{B_m}{C+B_m}S+\beta_2(I+\sigma A)S-(\rho+\mu)E\\(1-\theta)\rho E-(\delta+\gamma_1+\xi u_2+\mu)A\\\theta\rho E-(\delta+\gamma_2+\xi u_2+\mu)I\\(\gamma_1+\xi u_2)A+(\gamma_2+\xi u_2)I-(\alpha+\mu)R\\\eta(A+I)-\mu_b B_m\end{bmatrix}. \tag{5}$$

Then, the equation (5) can be written as $f(t,x,u)=f_1(t,x)+f_2(t,x)u$, where

$$f_1(t,x)=\begin{bmatrix}\Pi+\alpha R-\left(\beta_1\frac{B_m}{C+B_m}+\beta_2(I+\sigma A)+\mu\right)S\\\left(\beta_1\frac{B_m}{C+B_m}+\beta_2(I+\sigma A)\right)S-(\rho+\mu)E\\(1-\theta)\rho E-(\delta+\gamma_1+\mu)A\\\theta\rho E-(\delta+\gamma_2+\mu)I\\\gamma_1 A+\gamma_2 I-(\alpha+\mu)R\\\eta(A+I)-\mu_b B_m\end{bmatrix},\quad f_2(t,x)=\begin{bmatrix}\beta_1\frac{B_m}{C+B_m}S & 0\\-\beta_1\frac{B_m}{C+B_m}S & 0\\0 & -\xi A\\0 & -\xi I\\0 & \xi(A+I)\\0 & 0\end{bmatrix}.$$

From Euclidean norm of a matrix in [6,38], we obtain,

$$\| f(t,x,u)\|\leq\| f_1(t,x)\|+\| f_2(t,x)\|\| u\|\leq\max\{C_0,D\}(1+\| u\|),$$

where C_0 and D are positive constants given by

$$C_0=\frac{\Pi}{\mu}\sqrt{c_1\left(1+\Pi+\Pi^2\right)},\ \text{ and } D=\frac{\Pi}{\mu}\sqrt{\max\{d_1,d_2,d_3\}\left(1+\Pi+\Pi^2\right)}.$$

With

$$c_1=2(\beta_1^2+3\xi^2),\ \ d_1=\beta_1^2+(\alpha+\mu)^2+(\rho-\rho\theta)^2+\rho^2\theta^2+(\gamma_1+\gamma_2)^2+4\eta,$$
$$d_2=\frac{2\beta_1\beta_2(1+\sigma)}{\mu},\ \ d_3=\frac{\beta_2^2(1+\sigma)^2}{\mu^2}.$$

(iii) Let $y=(A,I)$ and $a,b\in U_0$, such that $a=(a_1,a_2)$ and $b=(b_1,b_2)$. The integrand of the objective functional in the equation (3) is the Lagrangian of the form denoted by $L(t,y,u)$ defined as

$$L(t,y,u)=L_1(t,y)+L_2(t,u), \tag{6}$$

where, $L_1(t,y)=w_1A+w_2I$, $L_2(t,u)=\frac{w_3}{2}u_1^2+\frac{w_4}{2}u_2^2$. It suffices to show that the function $L_2(t,u)$ is convex on the control set U_0. Thus, we need to show that

$$L(t,y,\phi a+(1-\phi)b)\leq\phi L(t,y,a)+(1-\phi)L(t,y,b),\ \forall\phi\in[0,1].$$

The equation (6) gives,

$$\begin{aligned}L(t,y,\phi a+(1-\phi)b)&=L_1(t,y)+L_2(t,\phi a+(1-\phi)b),\\&=L_1(t,y)+\frac{1}{2}\sum_{k=1}^{2}w_k\left(\phi a_k+(1-\phi)b_k\right)^2,\\&=L_1(t,y)+\frac{1}{2}\phi^2\sum_{k=1}^{2}w_k a_k^2+(1-\phi)\phi\sum_{k=1}^{2}w_k a_k b_k+\frac{1}{2}(1-\phi^2)\sum_{k=1}^{2}w_k a_k^2,\end{aligned}$$

and

$$\begin{aligned}\phi L(t,y,a)+L(t,y,(1-\phi)b)&=\phi\left(L_1(t,y)+L_2(t,a)\right)+(1-\phi)\left(L_1(t,y)+L_2(t,b)\right),\\&=L_1(t,y)+\frac{1}{2}\phi\sum_{k=1}^{2}w_k a_k^2+\frac{1}{2}(1-\phi)\sum_{k=1}^{2}w_k b_k^2.\end{aligned}$$

Since $\phi^2 \leq \phi \ \forall \phi \in [0,1]$, it follows that

$$L\big(t,y,\phi a+(1-\phi)b\big)-\Big(\phi L(t,y,a)+(1-\phi)L(t,y,b)\Big)=\frac{1}{2}(\phi^2-\phi)\sum_{k=1}^{2}w_k\Big(a_k-b_k\Big)^2\leq 0.$$

As a result, the function $L_2(t,u)$ is convex on U_0.

(iv) Using the equation (6), the last hypothesis is shown as follows:

$$L(t,y,u)=L_1(t,y)+\frac{1}{2}\sum_{k=1}^{2}w_k u_k^2\geq\frac{1}{2}\sum_{k=1}^{2}w_k u_k^2\geq\alpha_1\left(\sum_{k=1}^{2}\mid u_k\mid^2\right)^{\frac{\alpha_3}{2}}-\alpha_2,$$

where, $\alpha_1=\frac{1}{2}\min\{w_3,w_4\},\alpha_2>0$, and, $\alpha_3=2$.

3.3. Characterization of the optimal controls

To formulate an optimality system we need to generate the necessary conditions that the optimal control doublet and state must satisfy. Such conditions are generated from the Pontryagin's maximum principle (PMP) [37]. This principle converts the system (2) together with (3) into a problem of minimizing point-wise, with respect to controls u_1 and u_2, a Hamiltonian function, H, which is defined by

$$\begin{aligned}H=w_1A+w_2I+\frac{1}{2}\sum_{k=1}^{2}w_ku_k^2&+\lambda_1\left[\Pi+\alpha R-\left((1-u_1)\beta_1\frac{B_m}{C+B_m}+\beta_2(I+\sigma A)+\mu\right)S\right]\\&+\lambda_2\left[(1-u_1)\beta_1\frac{B_m}{C+B_m}S+\beta_2(I+\sigma A)S-(\rho+\mu)E\right]\\&+\lambda_3\left[(1-\theta)\rho E-(\delta+\gamma_1+\xi u_2+\mu)A\right]\\&+\lambda_4\left[\theta\rho E-(\delta+\gamma_2+\xi u_2+\mu)I\right]\\&+\lambda_5\left[(\gamma_1+\xi u_2)A+(\gamma_2+\xi u_2)I-(\alpha+\mu)R\right]\\&+\lambda_6\left[\eta(A+I)-\mu_bB_m\right],\end{aligned}\tag{7}$$

where, $\lambda_1,\lambda_2,\lambda_3,\lambda_4,\lambda_5$ and λ_6 are the adjoint variables associated with their respective state variables. The PMP [37] and the existence of the optimal control from [see Theorem 4.1, [17]] can be used to obtain the following theorem.

Theorem 3.2. *If $\Phi^*=(S^*,E^*,A^*,I^*,R^*,B_m^*)$ and $u^*=(u_1^*,u_2^*)$ are optimal state and optimal control solutions for the optimal problem (3), respectively, then, there exist six adjoint variables $\lambda_1,\lambda_2,\lambda_3,\lambda_4,\lambda_5$ and λ_6 that satisfy the adjoint system given by*

$$\begin{aligned}\frac{d\lambda_1}{dt}&=\big(\lambda_1-\lambda_2\big)\left((1-u_1)\beta_1\frac{B_m}{C+B_m}+\beta_2(I+\sigma A)\right)+\lambda_1\mu,\\\frac{d\lambda_2}{dt}&=\lambda_2(\rho+\mu)-\lambda_3(1-\theta)\rho-\lambda_4\theta\rho,\\\frac{d\lambda_3}{dt}&=-w_1+(\lambda_1-\lambda_2)\beta_2\sigma S+\lambda_3(\delta+\gamma_1+\mu+\xi u_2)-\lambda_5(\gamma_1+\xi u_2)-\lambda_6\eta,\\\frac{d\lambda_4}{dt}&=-w_2+(\lambda_1-\lambda_2)\beta_2S+\lambda_4(\delta+\gamma_2+\mu+\xi u_2)-\lambda_5(\gamma_2+\xi u_2)-\lambda_6\eta,\\\frac{d\lambda_5}{dt}&=-\lambda_1\alpha+\lambda_5(\alpha+\mu),\\\frac{d\lambda_6}{dt}&=(\lambda_1-\lambda_2)(1-u_1)\frac{\beta_1C}{(C+B_m)^2}S+\lambda_6\mu_b,\end{aligned}\tag{8}$$

with transversality conditions,

$$\lambda_k(T)=0,k=1,2,...,6.$$

Furthermore, the optimal controls u_1^* and u_2^* are characterized by

$$u_1^*=min\left\{1,max\left\{\frac{(\lambda_2-\lambda_1)\beta_1S\frac{B_m}{C+B_m}}{w_3},0\right\}\right\},\quad u_2^*=min\left\{1,max\left\{\frac{\xi A(\lambda_3-\lambda_5)+\xi I(\lambda_4-\lambda_5)}{w_4},0\right\}\right\}.\tag{9}$$

Proof. We apply PMP in order to obtain the adjoint relations, the transversality conditions and the optimal control doublet. By taking partial derivatives of the formulated Hamiltonian in the equation (7) with respect to the state variables S,E,A,I,R and B_m,

Table 1
Values and description of parameters of the model.

Parameter	Description	Value	Unit	Source
Π	Human recruitment rate	$\mu \times N0$	Humans day^{-1}	[14,45]
β_1	Human transmission rate due to pathogen	0.0999	Day^{-1}	Assumed
β_2	Human transmission rate due to A & I	0.0004	(Humans day)$^{-1}$	Assumed
θ	Probability of progress of E to I	0.5125	Dimensionless	Assumed
μ	Natural death rate of humans	$\frac{1}{65\times365}$	Day^{-1}	[45]
δ	Disease-induced death rate of A & I	0.0732	Day^{-1}	[14,45]
γ_1	Recovery rate from A	0.0248	Day^{-1}	[14,29]
γ_2	Recovery rate from I	0.0157	Day^{-1}	[14,29]
ρ	The progression rate of E to A & I	0.088	Day^{-1}	[14,44]
σ	Reduction rate of infectivity A	0.0493	Dimensionless	Assumed
α	Disease waning immunity	0.0726	Day^{-1}	Assumed
η	Rate at which bacteria increase by A & I	0.13	$\frac{\text{No. of } B.\ pseudomallei\ \text{cell}}{\text{Humans day}}$	[44]
μ_b	Natural death rate of bacteria	0.0185	Day^{-1}	[14,44]
C	Concentration of *B. pseudomallei*	5000	No. of *B. pseudomallei* cell	Assumed

as follows; $\frac{d\lambda_1}{dt} = -\frac{\partial H}{\partial S}, \frac{d\lambda_2}{dt} = -\frac{\partial H}{\partial E}, \frac{d\lambda_3}{dt} = -\frac{\partial H}{\partial A} =, \frac{d\lambda_4}{dt} = -\frac{\partial H}{\partial I}, \frac{d\lambda_5}{dt} = -\frac{\partial H}{\partial R}, \frac{d\lambda_6}{dt} = -\frac{\partial H}{\partial B_m},\ \lambda_k(T) = 0, k = 1, 2, ..., 6,$ yields the adjoint system given in the equation (8).

Finally, the characterization of optimal controls can be derived from H in (7) by using the optimal condition for each control measure u_i, where $0 < u_i < 1$, for $i = 1, 2$. Thus,

$$\frac{\partial H}{\partial u_i} = 0, \text{ for } i = 1, 2 \ (\textbf{optimal condition}) \tag{10}$$

Solving the equation (10) for optimal controls u_1^* and u_2^* we obtain the following characterization.

$$u_1^* = \frac{(\lambda_2 - \lambda_1)\beta_1 S \frac{B_m}{C+B_m}}{w_3}, \quad u_2^* = \frac{\xi A(\lambda_3 - \lambda_5) + \xi I(\lambda_4 - \lambda_5)}{w_4}.$$

Since the two control measures have lower bounds zero and upper bounds 1, we have

$$u_1^* \in u \Rightarrow u_1^* = \begin{cases} 0, & \text{if } \Psi_1 \le 0, \\ \Psi_1, & \text{if } 0 < \Psi_1 < 1, \\ 1, & \text{if } \Psi_1 \ge 1. \end{cases} \quad \text{and} \quad u_2^* \in u \Rightarrow u_2^* = \begin{cases} 0, & \text{if } \Psi_2 \le 0, \\ \Psi_2, & \text{if } 0 < \Psi_2 < 1, \\ 1, & \text{if } \Psi_2 \ge 1, \end{cases}$$

where, $\Psi_1 = \frac{(\lambda_2-\lambda_1)\beta_1 S \frac{B_m}{C+B_m}}{w_3}, \Psi_2 = \frac{\xi A(\lambda_3-\lambda_5)+\xi I(\lambda_4-\lambda_5)}{w_4}$. Therefore, in compact notation the optimal controls u_1^* and u_2^* given in the equation (9) are characterized by

$$u_1^* = \min\{1, \max\{\Psi_1, 0\}\}, \quad u_2^* = \min\{1, \max\{\Psi_2, 0\}\}.$$

4. Numerical results and cost-effectiveness analysis

4.1. Numerical methods

We compare the numerical results of the autonomous model (1) and the controlled model (2) to evaluate the effectiveness of the control strategies in controlling the spread of the disease. To perform this, we used an iterative method so-called Forward-Backward Sweep method (FBSM) based on the fourth-order Runge-Kutta Method (RKM-4) in the Matlab program, described in detail in a book by Lenhart and Workman [26]. The process begins with an initial guess for the control variables, we solve the state equations over the interval [0, 250] using forward RKM-4. Then, we apply the backward RKM-4 to solve the adjoint equations by using the current iteration solution of (2). The control values are updated by averaging the previous value and the new value from the control characterization (9), and the process is repeated until the required convergence occurs. The parameters values used in the simulations are given in Table 1.

For those parameters values the basic reproduction number is obtained as $R_0 \approx 2.0326 > 1$, the unique positive endemic equilibrium $\varepsilon_{12}^* = \left(235.5204, 1.6735, 0.8452, 0.7296, 0.4297, 13.833\right)$, with initial conditions of state variables $S(0) = 452.09, E(0) = 48, A(0) = I(0) = 10, R(0) = 0, Bm(0) = 200$. In addition, the weight constants values and the control rate of treatment are chosen as; $w_1 = 10, w_2 = 10, w_3 = 8, w_4 = 10, \xi = 0.75$. It is important to note that, the choice of treatment control rate ($\xi = 0.75$) is based on the

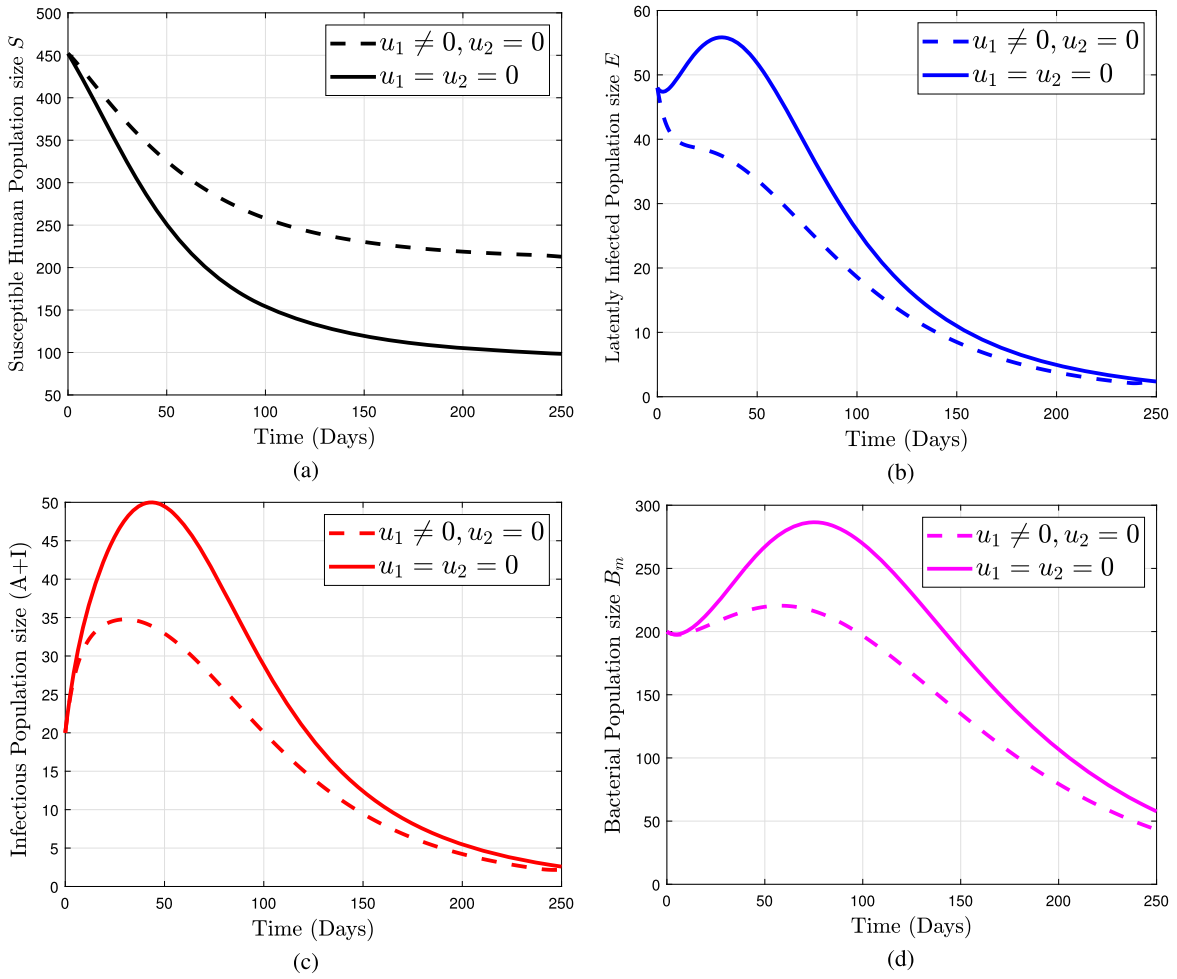

Fig. 2. Simulations of the model system (2) showing the effects of the "Strategy A"; (a) dynamics of susceptible class with and without optimal control u_1, (b) dynamics of latently infected class with and without optimal control u_1, (c) dynamics of infectious classes $(A + I)$ with and without optimal control u_1 and (d) dynamics of the bacterial population with and without optimal control u_1.

melioidosis infection relapse cases, which varies from 13% to 23% in patients [23,39] (see details in the introduction section of the paper).

4.2. Numerical results

To illustrate the impact of different optimal control strategies for melioidosis epidemic, we implemented all the three possible optimal strategies of alternative combinations of the control measures, u_1 and u_2:

- Strategy A: Preventive measure only $(u_1 \neq 0, u_2 = 0)$,
- Strategy B: Treatment of infectious individuals (asymptomatic and symptomatic) $(u_2 \neq 0, u_1 = 0)$,
- Strategy C: Combination of both preventive measure and treatment control $(u_1 \neq 0, u_2 \neq 0)$.

4.2.1. Strategy A: Preventive measure only $(u_1 \neq 0, u_2 = 0)$

This strategy implements the preventive measure u_1 only. As shown, in Fig. 2 (a), the number of susceptible individuals decreases without strategy A compared to the number of susceptible individuals with the strategy. On the other hand, in Fig. 2 (b) the size of latently infected individuals decreases rapidly when the strategy is implemented throughout the intervention period, while in the absence of the strategy the number of latently infected individuals increases rapidly to peak in the first 35 days and then diminishes slowly in rest of time interval. In Fig. 2 (c), it can be seen that the size of infectious individuals (asymptomatic + symptomatic) increases more sharply without preventive measures than the number of infectious individuals with the preventive measure in the first 50 days, while the size of infectious individuals (asymptomatic + symptomatic) decreases more rapidly with preventive measure than the number of infectious individuals without preventive measure in the rest of interventions days. A similar situation is observed in Fig. 2 (d) for *Burkholderia pseudomallei* population. Further, in Fig. 5 (a), the control profile for the "strategy A" shows that the

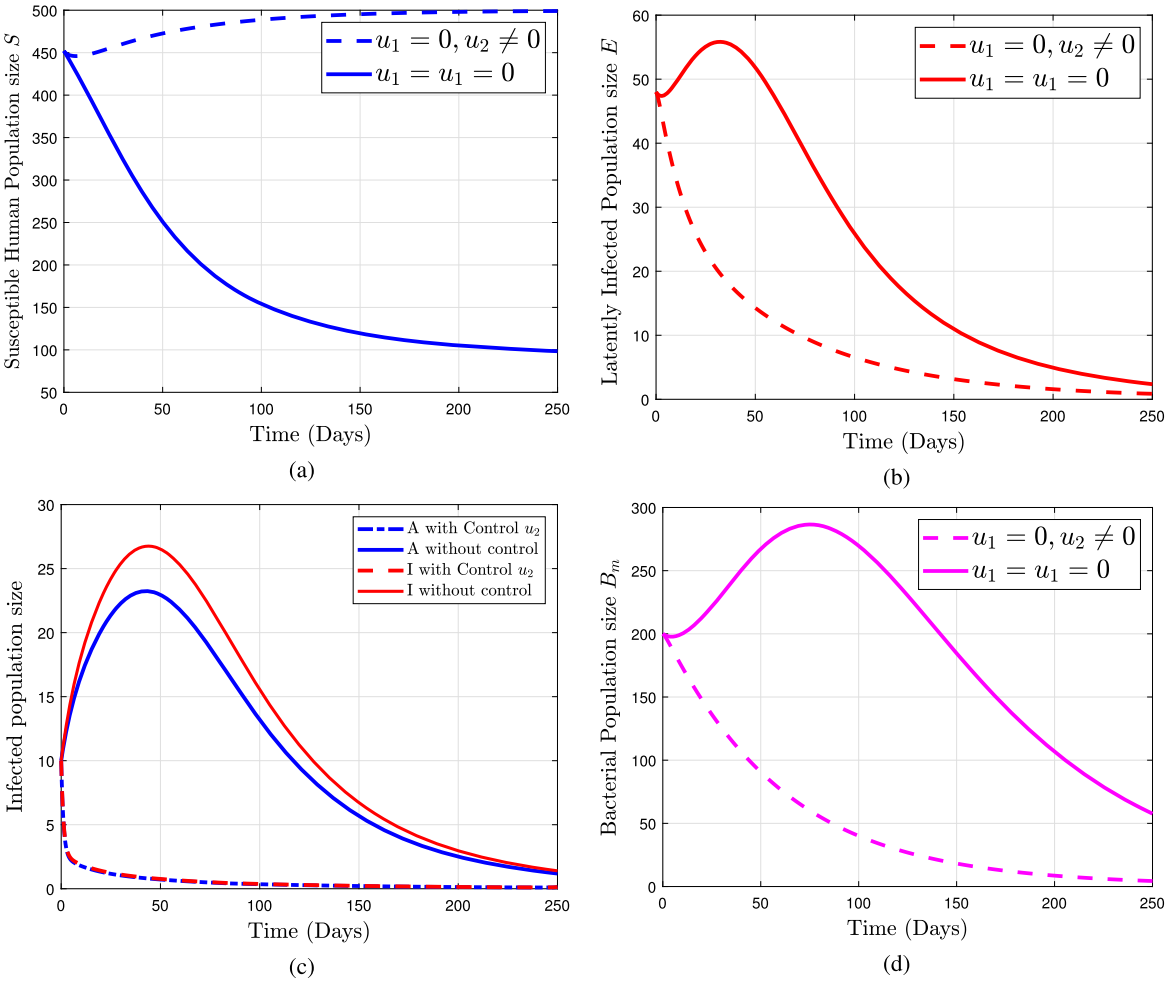

Fig. 3. Simulations of the model system (2) showing the effect of the "Strategy B"; (a) dynamics of susceptible class with and without optimal control u_2, (b) dynamics of latently infected class with and without optimal control u_2, (c) dynamics of infectious classes (A & I) with and without optimal control u_2 and (d) dynamics of bacterial population with and without optimal control u_2.

preventive effort u_1 should be implemented at maximum coverage (100%) for the initial 236.8 days. After that period, preventive effort should be gradually reduced to the lower bound for the rest of the simulation time.

4.2.2. Strategy B: Treatment control only ($u_2 \neq 0, u_1 = 0$)

This strategy is applied to the optimal use of treatment control u_2 for infectious individuals. In Fig. 3(a), we observed that the susceptible human population gradually increases in size when control measure u_2 is implemented, in contrast, the number of susceptible individuals decreases rapidly in the absence of control measure. From Figs. 3 (b) - 3 (d) we observed that the number of latently infected humans, infectious individuals (asymptomatic + symptomatic) and the size of pathogen population decreased dramatically when the optimal control is implemented throughout the simulation period. This illustrates that the number of infective classes ($E, A,$ & I), and B_m could be vanished when the strategy is implemented. In general, from Figs. 3 (a) - 3 (d), we observed that this strategy is more effective in reducing the spread of disease in the infected population than strategy A. Furthermore, the control profile of this strategy in Fig. 5 (b) shows that the treatment control u_2 should be maintained at the upper bound (100%) for the first 84 days and subsequently it should be gradually reduced to zero (lower bound) for the rest of the simulation time.

4.2.3. Strategy C: Combination of both preventive and treatment measures ($u_1 \neq 0, u_2 \neq 0$)

This strategy implements both intervention measures $u_1(t)$ and $u_1(t)$. In Fig. 4 (a), we noted that the population's number of susceptible individuals gradually rises when the optimal strategy C is present. Conversely, in the absence of the strategy, the number of susceptible individuals declines rapidly over the simulation period. In Fig. 4 (b) - 4 (d), we noted that the size of latently infected humans, infectious individuals (asymptomatic + symptomatic), and the size of the pathogen population diminished more rapidly when the strategy C implemented. The size of latently infected and infectious individuals increase sharply to a peak point in the first 40 days and then decrease slowly in the remaining simulation period in the absence of optimal control as shown in Figs. 4 (b)

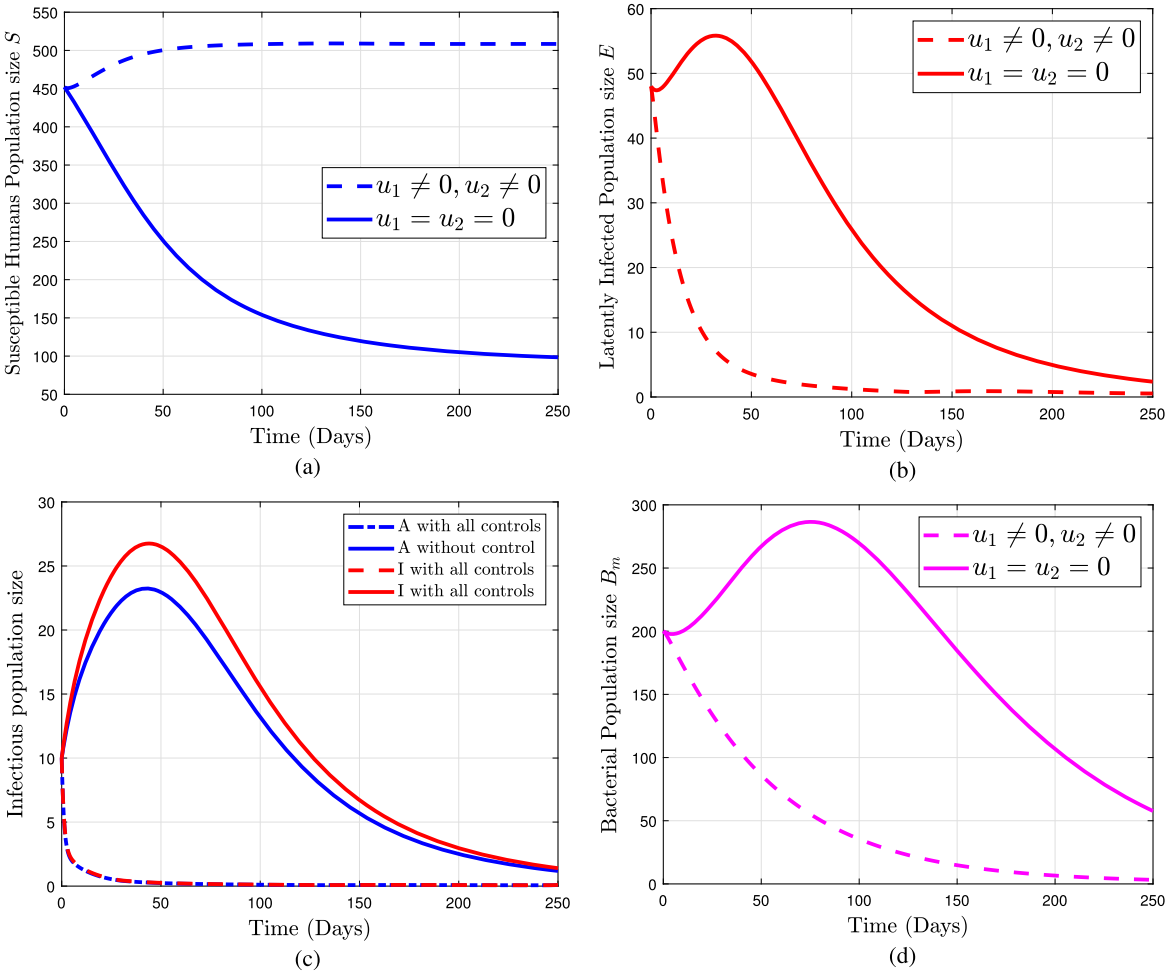

Fig. 4. Simulations of the model system (2) showing the effect of the "Strategy C"; (a) dynamics of susceptible class with and without combined optimal controls u_1 & u_2, (b) dynamics of latently infected class with and without combined optimal controls u_1 & u_2, (c) dynamics of infectious classes (A & I) with and without combined optimal controls u_1 & u_2 and (d) dynamics of bacterial population with and without combined optimal controls u_1 & u_2.

and 4 (c). The same situation is observed in Fig. 4 (d) for the pathogen population. Further, in Fig. 5 (c), the control profile for the "strategy C" indicates the following:

(i) The preventive effort should be maintained at the upper bound (100%) for the first 126 days.
(ii) The treatment control should be kept at the upper bound (100%) for the first 28 days.

After the specified durations, both controls should be gradually reduced to the lower bound for the rest of the simulation time.

4.2.4. Comparison of the three control strategies

In this section, we compare the effectiveness of the three strategies A, B and C, to determine the most effective strategy, typically for minimizing the infectious classes. Further, the comparison of the simulations of the model with and without the strategies for populations of susceptible humans, latently infected individuals, infectious individuals ($A + I$) and bacteria are demonstrated in Figs. 6(a) - 6(d). From Fig. 6(a), it can be seen that strategy C is the most effective in reducing the size of the susceptible class getting infected by the disease, followed by strategies B and A, respectively. While in Fig. 6(b) we observed that strategy C is the most effective to reduce the size of the latently infected class compared to strategies A and B. Likewise, Fig. 6(c) shows that strategy C has the highest number of infectious averted humans ($A + I$) followed by strategy B and then strategy A. Moreover, strategy C is most effective in reducing the growth of bacterial population in the environment as indicated in Fig. 6(d).

In view of the numerical simulations of the three control strategies, the implementation of the control strategies B and C dramatically minimizes the size of infectious classes in the population as well as the concentration of bacteria in the environment as illustrated in Figs. 3(c) & 3 (d) and in Figs. 4(c) & 4 (d). Therefore, these control strategies target-fully reduce disease transmission in the human population. While, the numerical results indicate that strategy C is more effective in diminishing the number of infectious classes compared to strategy B regardless of the costs of the optimal control strategies as confirmed in Fig. 6. These results agree

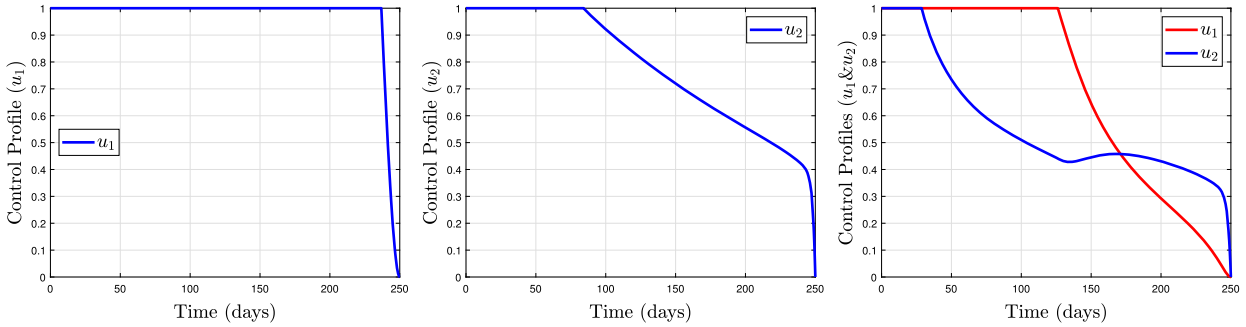

Fig. 5. Simulations showing the control profiles of the three strategies (A, B & C).

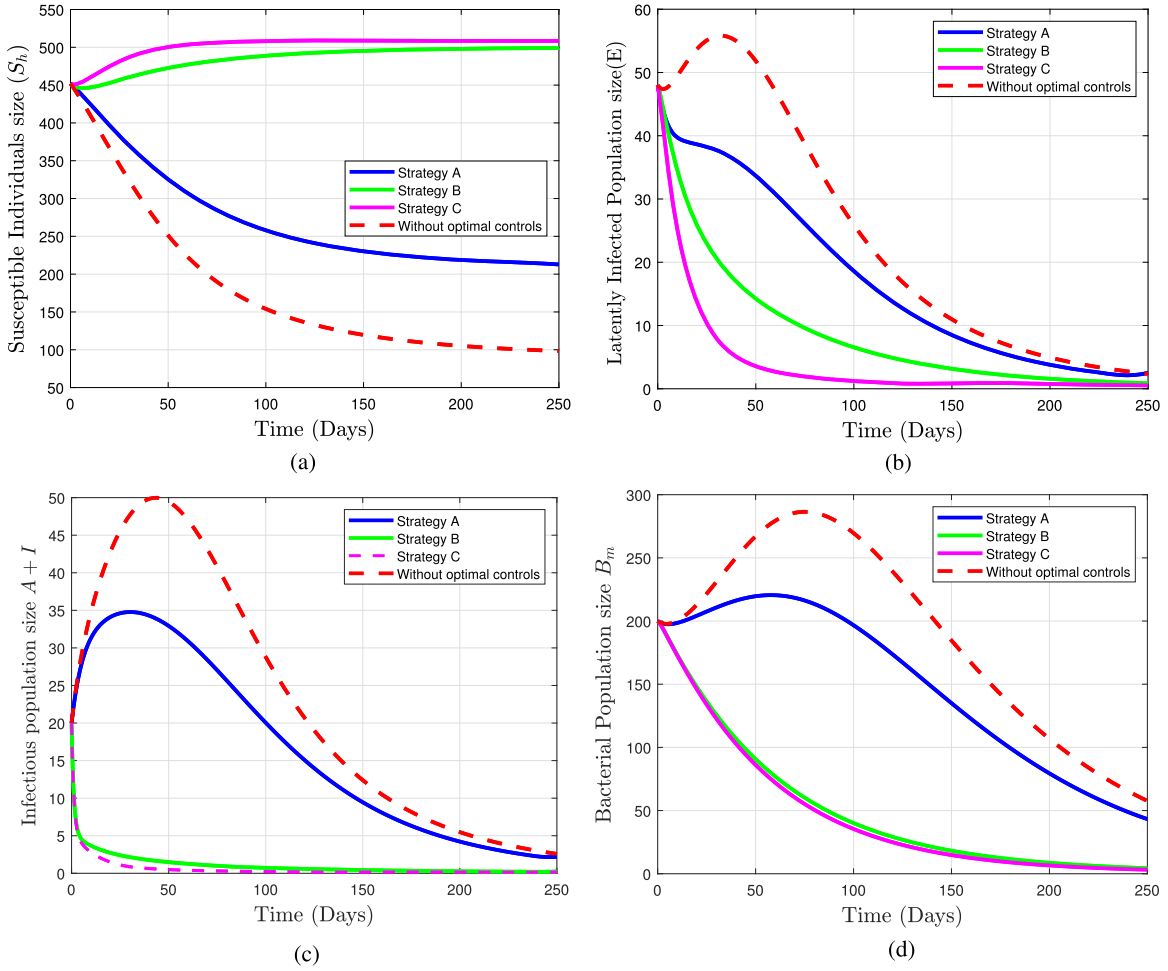

Fig. 6. Simulations of the model system (2) showing the comparison of the three optimal control Strategies ($A, B\&C$) with the autonomous system (1); (a) the effectiveness of all three strategies with the autonomous system (1) for susceptible humans, (b) the effectiveness of all three strategies with the autonomous system (1) for latently infected individuals, (c) the effectiveness of all three strategies with the autonomous system (1) for infectious individuals ($A\&I$) and (d) the effectiveness of all three strategies with the autonomous system (1) for the bacterial population.

with the results obtained in section 3.1. Furthermore, the cost profiles for each of the three strategies are depicted in Figs. 7(a), 7(b) and 7(c). To determine the most cost-effective strategy among the three control strategies, we carry out a cost-effectiveness analysis in the next section.

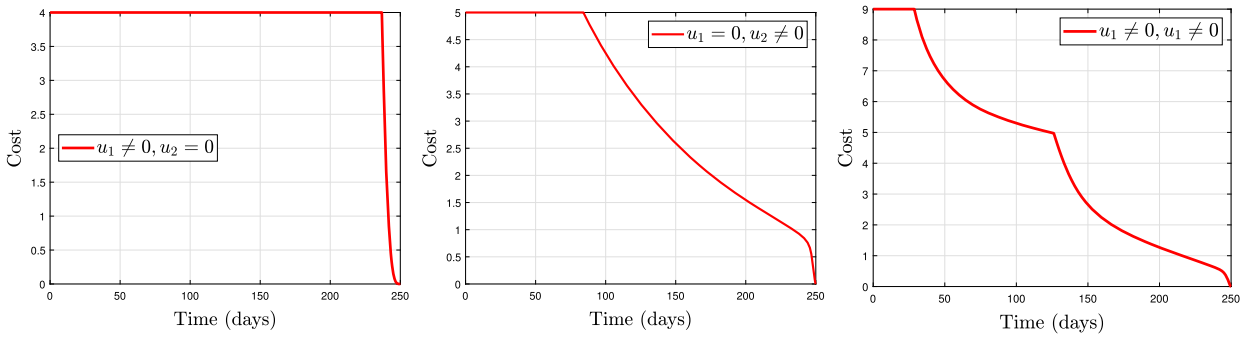

(a) Cost profile of Strategy A (b) Cost profile of Strategy B (c) Cost profile of Strategy C

Fig. 7. Simulations showing the cost profiles of the three Strategies (A, B & C).

4.3. Cost-effectiveness analysis

The cost-effective analysis is one of most economical evaluation tool used to measure mainly the costs of alternative interventions and therefore, it is used to compare and assess how the greatest health benefits can be generated and to rank the implemented strategies in-terms of their cost [5].

In this section two approaches, namely the average cost-effectiveness ratio (ACER) and the incremental cost-effectiveness ratio (ICER) are performed to obtain the most cost-effective strategy among the three alternative strategies (A, B, and C), using the ideas in [1,2,15,18,31].

4.3.1. Average cost-effectiveness ratio (ACER)

The average cost-effectiveness ratio (ACER) of an optimal control strategy S is given by the formula:

$$\text{ACER(S)} = \frac{\text{Total cost produced by the strategy S}}{\text{Total number of infection averted by the strategy S}} \tag{11}$$

It is concerned with a single optimal strategy and measures the strategy against baseline option. The total number of infection averted is given as the difference between the total number of infectious individuals over the simulation period without control and the number of total infectious individuals with control. A strategy with the least ACER value is the most cost-effective measure.

The total number of symptomatic infection averted during the intervention period is approximated from;

$$T_I = \int_0^{250} I(t)\,dt - \int_0^{250} I^*(t)\,dt \tag{12}$$

where, T_I total number of symptomatic infections averted,

$$\int_0^{250} I(t)\,dt$$

represents the total symptomatic infectious cases without control over [0,250], and $I^*(t)$ is the optimal solution associated to the susceptible infections. In the same manner, the total number of asymptomatic infection averted during the intervention period is approximated from;

$$T_A = \int_0^{250} A(t)\,dt - \int_0^{250} A^*(t)\,dt \tag{13}$$

It is important to note that the total number of infections averted for the strategies is calculated using the MATLAB program, based on the above equations (12) and (13). The total number of infections averted for each strategy is determined by taking the average value of both the total number of symptomatic infections averted and the total number of asymptomatic infections averted by the strategy. These values are provided in the second column of Table 2.

While the total cost associated to the intervention is approximated from

$$T_C = \frac{1}{2}\int_0^{250} \left(w_3 u_1^2 + w_4 u_2^2\right) dt.$$

Specifically, the total cost produced by the strategy A, strategy B, and strategy C are, respectively, approximated as:

Table 2
Total infection averted, total cost produced by control strategies, ACER values and ICER values.

Strategy	Infection averted	Total Cost ($)	ACER values	ICER values
Strategy A	880.3	972.9036	1.1	1.1
Strategy B	2868.0042	934.3206	0.33	-0.0194
Strategy C	2940.8231	1219.6	0.4	3.9

$$T_{Ca} = \frac{1}{2}\int_0^{250}\left(w_3u_1^2\right)dt, \quad T_{Cb} = \frac{1}{2}\int_0^{250}\left(w_4u_2^2\right)dt, \quad \text{and} \quad T_{Cc} = \frac{1}{2}\int_0^{250}\left(w_3u_1^2 + w_4u_2^2\right)dt, \quad \text{using MATLAB.}$$

The ACER for each of the strategies is calculated using the equation (11) and the values are given in fourth column of Table 2. From the Table 2, we conclude that the strategy B is the most cost effective of all the three possible strategies under consideration for this particular investigation.

4.3.2. The incremental cost-effectiveness ratio (ICER)

The incremental cost-effectiveness ratio is given by the formula:

$$\text{ICER} = \frac{\text{Difference in total intervation costs between strategies}}{\text{Difference in the total number of infection averted between strategies}} \tag{14}$$

The ICER's numerator includes (if applicable) the differences in the cost of interventions, costs of disease averted or costs of prevented cases among others. While the denominator given in the equation (14) determines the differences in health outcomes which include the total number of infections averted or the number of susceptibility cases prevented. To implement the ICER, we simulate the model using the three interventions strategies. Based on these simulation results of the optimal control problem, the intervention strategies are then ranked according to their increasing order of total number of infection averted. We have that strategy A averts the least number of the disease infections, followed by strategy B, and strategy C which averted the most number of infections as shown in Table 2. The ICER value for each strategy is computed using the equation (14) as follows:

$$\text{ICER(A)} = \frac{972.9036 - 0}{880.3 - 0} \approx 1.1, \quad \text{ICER(B)} = \frac{934.3206 - 972.9036}{2868.0042 - 880.3} \approx -0.0194,$$
$$\text{ICER(C)} = \frac{1219.6 - 934.3206}{2940.8231 - 2868.0042} \approx 3.9.$$

From ICER values of the strategies, we observed that ICER (C) is greater than ICER (A). It follows that, strategy C is more costly and less effective than strategy A. Therefore, it is better to remove strategy C from the list of alternative interventions and then the strategy A will be compared with the strategy B, by re-calculating ICER for each as follows.

$$\text{ICER(A)} = \frac{972.9036 - 0}{880.3 - 0} \approx 1.1, \quad \text{ICER(B)} = \frac{934.3206 - 972.9036}{2868.0042 - 880.3} \approx -0.0194.$$

The result of comparison between two strategies, indicates that strategy B is strongly dominated by the strategy A. Thus, the strategy A is more costly and less effective than the strategy B. Consequently, the strategy B (treatment control) is most cost-effective of all the strategies for control of melioidosis infection under consideration for this particular study. This result agrees with the result of the ACER method obtained earlier. Furthermore, figures for the total number of infections averted, the total cost, ACER values and ICER values of the strategies are given below in Fig. 8, Fig. 9, Fig. 10 and Fig. 11, respectively.

5. Conclusion

In this work, we formulated and analyzed an optimal control problem that demonstrates the effectiveness of different control functions for eliminating the epidemic, as well as the overall cost-effectiveness of the introduced controls. The formulated optimal control model is a continuation of the basic model presented in [14]. The model is extended by incorporating two time-dependent control variables, namely personal prevention $u_1(t)$ and treatment control $u_2(t)$. The effect of these control variables on the basic reproduction of the non-autonomous system is illustrated graphically in Fig. (1), and the results are discussed. The standard results for the existence and characterization of optimal controls are established to obtain the optimality system for the optimal control problem. The optimality system is simulated by using the forward-backward sweep method in the MATLAB program to assess the impact of the three alternative optimal strategies by comparing them without controls on the transmission dynamics of the melioidosis epidemic: Strategy A-implementation of personal prevention control only, Strategy B-implementation of treatment control only, and Strategy C-implementation of the combination of both personal prevention and treatment controls. The numerical results show that the Strategy C will effectively reduce the number of infected individuals (both asymptomatic and symptomatic) in the population as demonstrated in Figs. 4. Additionally, the Strategy B has also a significant impact in reducing the infected classes as depicted in Fig. 3. These results are confirmed quantitatively in terms of the total number of infections averted. It is observed that the Strategy C averted the highest number of infectious individuals, followed by the Strategy B, and the Strategy A, which averted the least number

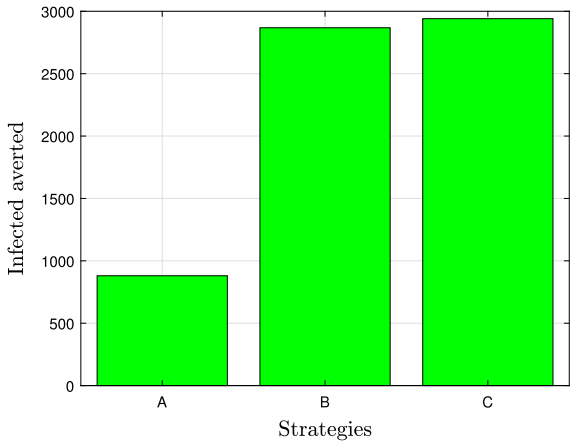

Fig. 8. Total number of infected averted for control strategies.

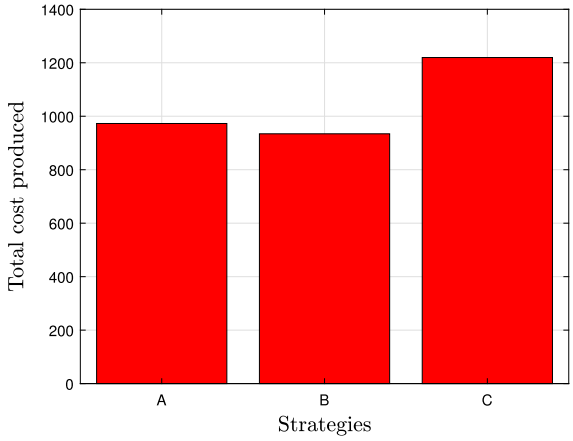

Fig. 9. Total cost produced by control strategies.

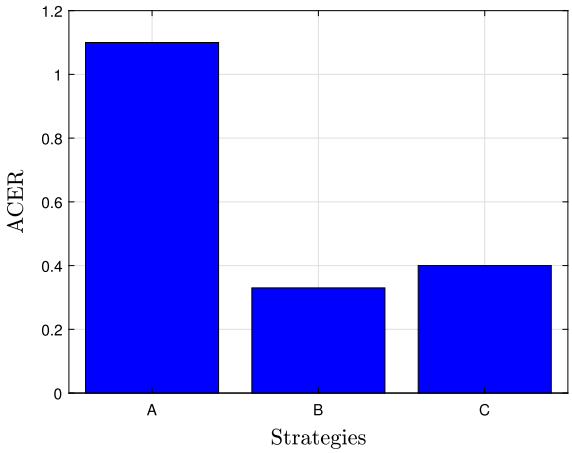

Fig. 10. ACER values for all strategies.

of infectious individuals, as demonstrated in Table 2 and Fig. (8). However, the cost-effectiveness analysis carried out reveals that the Strategy B is the most cost-effective intervention strategy of all the three intervention strategies as confirmed quantitatively by ACER and ICER in Table 2, and in Figs. 10 and 11. This shows that the treatment control strategy should be recommended to diminish the spread of the disease when available resources are limited. Therefore, using all the control strategies as suggested in [44] is not recommended regarding the costs of the optimal control strategies.

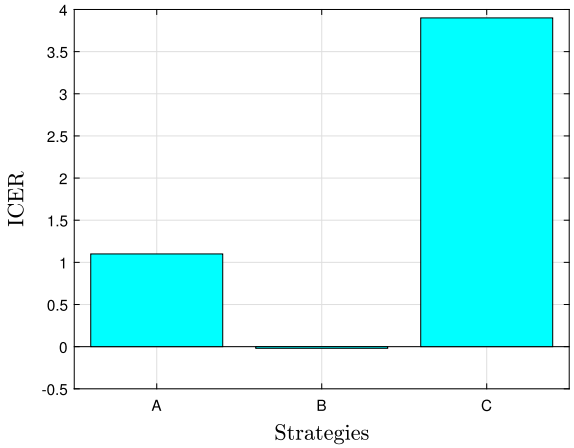

Fig. 11. ICER values for all strategies.

Funding statement

This research did not receive any specific grant from funding agencies in the public, commercial, or not-for-profit sectors.

Additional information

No additional information is available for this paper.

CRediT authorship contribution statement

Habtamu Ayalew Engida: Writing – review & editing, Writing – original draft, Supervision, Software, Methodology, Investigation, Formal analysis, Conceptualization. **Duncan Kioi Gathungu:** Visualization, Supervision, Resources, Methodology. **Melkamu Molla Ferede:** Visualization, Supervision, Resources. **Malede Atnaw Belay:** Visualization, Supervision, Resources. **Patiene Chouop Kawe:** Visualization, Supervision, Resources. **Bilali Mataru:** Visualization, Supervision, Resources.

Declaration of competing interest

The authors declare that they have no known competing financial interests or personal relationships that could have appeared to influence the work reported in this paper.

Data availability

Data included in this article/supplementary material/referenced in the article.

References

[1] Folashade B. Agusto, Ibrahim M. ELmojtaba, Optimal control and cost-effective analysis of malaria/visceral leishmaniasis co-infection, PLoS ONE 12 (2) (2017) e0171102.
[2] J.O. Akanni, F.O. Akinpelu, S. Olaniyi, A.T. Oladipo, A.W. Ogunsola, Modelling financial crime population dynamics: optimal control and cost-effectiveness analysis, Int. J. Dyn. Control 8 (2) (2020) 531–544.
[3] Dipo Aldila, Michellyn Angelina, Optimal control problem and backward bifurcation on malaria transmission with vector bias, Heliyon 7 (4) (2021) e06824.
[4] Mohammad R. Mohd Ali, Amira W. Mohamad Safiee, Padmaloseni Thangarajah, Mohd H. Fauzi, Alwi Muhd Besari, Nabilah Ismail, Chan Yean Yean, Molecular detection of leptospirosis and melioidosis co-infection: a case report, J. Infect. Public Health 10 (6) (2017) 894–896.
[5] Ali R. Ansari, Advances in Applied Mathematics, Springer, 2014, pp. 31–40.
[6] Joshua Kiddy K. Asamoah, Eric Okyere, Afeez Abidemi, Stephen E. Moore, Gui-Quan Sun, Zhen Jin, Edward Acheampong, Joseph Frank Gordon, Optimal control and comprehensive cost-effectiveness analysis for covid-19, Results Phys. (2022) 105177.
[7] Ammar Aziz, Bart J. Currie, Mark Mayo, Derek S. Sarovich, Erin P. Price, Comparative genomics confirms a rare melioidosis human-to-human transmission event and reveals incorrect phylogenomic reconstruction due to polyclonality, Microb. Genomics 6 (2) (2020).
[8] Tina J. Benoit, David D. Blaney, Jay E. Gee, Mindy G. Elrod, Alex R. Hoffmaster, Thomas J. Doker, William A. Bower, Henry T. Walke, Melioidosis cases and selected reports of occupational exposures to burkholderia pseudomallei—United States, 2008–2013, Morb. Mortal. Wkly. Rep., Surveill. Summ. 64 (5) (2015) 1–9.
[9] Arindam Chakravorty, Christopher H. Heath, Melioidosis: an updated review, Aust. J. Gen. Pract. 48 (5) (2019) 327–332.
[10] Sukanta Chowdhury, Lovely Barai, Samira Rahat Afroze, Probir Kumar Ghosh, Farhana Afroz, Habibur Rahman, Sumon Ghosh, Muhammad Belal Hossain, Mohammed Ziaur Rahman, Pritimoy Das, et al., The epidemiology of melioidosis and its association with diabetes mellitus: a systematic review and meta-analysis, Pathog. 11 (2) (2022) 149.
[11] Bart J. Currie, Mirjam Kaestli, A global picture of melioidosis, Nature 529 (7586) (2016) 290–291.

[12] David Dance, Treatment and prophylaxis of melioidosis, Int. J. Antimicrob. Agents 43 (4) (2014) 310–318.
[13] Subarna Dutta, Sabah Haq, Mohammad Rokibul Hasan, Jalaluddin Ashraful Haq, Antimicrobial susceptibility pattern of clinical isolates of burkholderia pseudomallei in Bangladesh, BMC Res. Notes 10 (1) (2017) 1–5.
[14] Habtamu Ayalew Engida, David Mwangi Theuri, Duncan Gathungu, John Gachohi, Haileyesus Tessema Alemneh, A mathematical model analysis of the human melioidosis transmission dynamics with an asymptomatic case, Heliyon (2022) e11720.
[15] Habtamu Ayalew Engida, David Mwangi Theuri, Duncan Kioi Gathungu, John Gachohi, Optimal control and cost-effectiveness analysis for leptospirosis epidemic, J. Biol. Dyn. 17 (1) (2023) 2248178.
[16] Shirley Hii Yi Fen, Sarunporn Tandhavanant, Rungnapa Phunpang, Peeraya Ekchariyawat, Natnaree Saiprom, Claire Chewapreecha, Rathanin Seng, Ekkachai Thiansukhon, Chumpol Morakot, Narongchai Sangsa, et al., Antibiotic susceptibility of clinical burkholderia pseudomallei isolates in northeast Thailand during 2015-2018 and the genomic characterization of β-lactam-resistant isolates, Antimicrob. Agents Chemother. (2021).
[17] W.H. Fleming, R.W. Rishel, G.I. Marchuk, A.V. Balakrishnan, A.A. Borovkov, V.L. Makarov, A.M. Rubinov, R.S. Liptser, A.N. Shiryayev, N.N. Krassovsky, et al., Applications of mathematics, in: Deterministic and Stochastic Optimal Control, 1975.
[18] Mini Ghosh, Samson Olaniyi, Olawale S. Obabiyi, Mathematical analysis of reinfection and relapse in malaria dynamics, Appl. Math. Comput. 373 (2020) 125044.
[19] Hans Heesterbeek, Roy M. Anderson, Viggo Andreasen, Shweta Bansal, Daniela De Angelis, Chris Dye, Ken T.D. Eames, W. John Edmunds, Simon D.W. Frost, Sebastian Funk, et al., Modeling infectious disease dynamics in the complex landscape of global health, Science 347 (6227) (2015).
[20] Herbert W. Hethcote, The mathematics of infectious diseases, SIAM Rev. 42 (4) (2000) 599–653.
[21] Karunanayake Panduka, Melioidosis: clinical aspects, Clin. Med. 22 (1) (2022) 6.
[22] A.K.T.M. Karunarathna, S.A. Mendis, W.P.D.P. Perera, Geethika Patabendige, A.S. Pallewatte, Aruna Kulatunga, A case report of melioidosis complicated by infective sacroiliitis in Sri Lanka, Trop. Dis. Travel Med. Vaccines 4 (1) (2018) 1–6.
[23] Paul Vijay Kingsley, Govindakarnavar Arunkumar, Meghan Tipre, Mark Leader, Nalini Sathiakumar, Pitfalls and optimal approaches to diagnose melioidosis, Asian Pac. J. Trop. Med. 9 (6) (2016) 515–524.
[24] Anuj Kumar, Prashant K. Srivastava, Vaccination and treatment as control interventions in an infectious disease model with their cost optimization, Commun. Nonlinear Sci. Numer. Simul. 44 (2017) 334–343.
[25] Sonu Lamba, Prashant K. Srivastava, Cost-effective optimal control analysis of a covid-19 transmission model incorporating community awareness and waning immunity, Comput. Math. Biophys. 11 (1) (2023) 20230154.
[26] Suzanne Lenhart, John T. Workman, Optimal Control Applied to Biological Models, CRC Press, 2007, pp. 5–33.
[27] Direk Limmathurotsakul, Nick Golding, David A.B. Dance, Jane P. Messina, David M. Pigott, Catherine L. Moyes, Dionne B. Rolim, Eric Bertherat, Nicholas P.J. Day, Sharon J. Peacock, et al., Predicted global distribution of burkholderia pseudomallei and burden of melioidosis, Nat. Microbiol. 1 (1) (2016) 1–5.
[28] Nantasit Luangasanatip, Stefan Flasche, David AB Dance, Direk Limmathurotsakul, Bart J. Currie, Chiranjay Mukhopadhyay, Tim Atkins, Richard Titball, Mark Jit, The global impact and cost-effectiveness of a melioidosis vaccine, BMC Med. 17 (1) (2019) 1–11.
[29] Wiriya Mahikul, Lisa J. White, Kittiyod Poovorawan, Ngamphol Soonthornworasiri, Pataporn Sukontamarn, Phetsavanh Chanthavilay, Graham F. Medley, Wirichada Pan-Ngum, Modelling population dynamics and seasonal movement to assess and predict the burden of melioidosis, PLoS Negl. Trop. Dis. 13 (5) (2019) e0007380.
[30] Prasanta R. Mohapatra, Baijayantimala Mishra, Burden of melioidosis in India and south Asia: challenges and ways forward, in: The Lancet Regional Health-Southeast Asia, 2022.
[31] Eric Okyere, Samson Olaniyi, Ebenezer Bonyah, Analysis of Zika virus dynamics with sexual transmission route using multiple optimal controls, Sci. Afr. 9 (2020) e00532.
[32] S. Olaniyi, K.O. Okosun, S.O. Adesanya, R.S. Lebelo, Modelling malaria dynamics with partial immunity and protected travellers: optimal control and cost-effectiveness analysis, J. Biol. Dyn. 14 (1) (2020) 90–115.
[33] Samson Olaniyi, Kazeem O. Okosun, Samuel O. Adesanya, Emmanuel A. Areo, Global stability and optimal control analysis of malaria dynamics in the presence of human travelers, Open Inf. Dis. J. 10 (1) (2018).
[34] Andrew Omame, Mujahid Abbas, Modeling sars-cov-2 and hbv co-dynamics with optimal control, Phys. A, Stat. Mech. Appl. 615 (2023) 128607.
[35] Andrew Omame, Mujahid Abbas, Chibueze P. Onyenegecha, Backward bifurcation and optimal control in a co-infection model for sars-cov-2 and zikv, Results Phys. 37 (2022) 105481.
[36] N.M. Phillips, A. Cervin, J. Earnshaw, H.E. Sidjabat, Melioidosis in a patient with chronic rhinosinusitis, J. Laryngol. Otolog 130 (S4) (2016) S60–S62.
[37] L.S. Pontryagin, V.G. Boltyanskii, R.V. Gamkrelidze, E.F. Mishchenko, The Maximum Principle. The Mathematical Theory of Optimal Processes, John Wiley and Sons, New York, 1962.
[38] Jhoana P. Romero-Leiton, J.M. Montoya-Aguilar, E. Ibargüen-Mondragón, An optimal control problem applied to malaria disease in Colombia, Appl. Math. Sci. 12 (6) (2018) 279–292.
[39] Brittany N. Ross, Julia N. Myers, Laura A. Muruato, Daniel Tapia, Alfredo G. Torres, Evaluating new compounds to treat burkholderia pseudomallei infections, Front. Cell. Infect. Microbiol. 8 (2018) 210.
[40] Oluwaseun Sharomi, Tufail Malik, Optimal control in epidemiology, Ann. Oper. Res. 251 (1–2) (2017) 55–71.
[41] Mandeep Singh, Mehvish Mahmood, Melioidosis: the great mimicker, J. Commun. Hosp. Int. Med. Perspect. 7 (4) (2017) 245–247.
[42] Akriti Srivastava, Prashant K. Srivastava, et al., Nonlinear dynamics of a siri model incorporating the impact of information and saturated treatment with optimal control, Eur. Phys. J. Plus 137 (9) (2022) 1–25.
[43] Wenyu Sun, Ya-Xiang Yuan, Optimization Theory and Methods: Nonlinear Programming, vol. 1, Springer Science & Business Media, 2006.
[44] Sunisa Tavaen, Ratchada Viriyapong, Global stability and optimal control of melioidosis transmission model with hygiene care and treatment, Int. J. Sci. 16 (2) (2019) 31–48.
[45] Yibeltal Adane Terefe, Semu Mitiku Kassa, Analysis of a mathematical model for the transmission dynamics of human melioidosis, Int. J. Biomath. 13 (07) (2020) 2050062.
[46] Pauline Van den Driessche, James Watmough, Reproduction numbers and sub-threshold endemic equilibria for compartmental models of disease transmission, Math. Biosci. 180 (1–2) (2002) 29–48.
[47] W. Joost Wiersinga, Harjeet S. Virk, Alfredo G. Torres, Bart J. Currie, Sharon J. Peacock, David A.B. Dance, Direk Limmathurotsakul, Melioidosis, Nat. Rev. Dis. Primers 4 (1) (2018) 1–22.